# Supplementary Materials for

## Immunological characteristics govern the transition of COVID-19 to endemicity

Jennie S. Lavine*, Ottar N. Bjornstad, Rustom Antia

*Corresponding author. Email: jslavin@emory.edu

Published 12 January 2021 on *Science* First Release
DOI: 10.1126/science.abe6522

**This PDF file includes:**



**Other Supplementary Material for this manuscript includes the following:**
(available at science.sciencemag.org/cgi/content/full/science.abe6522/DC1)

MDAR Reproducibility Checklist (.pdf)

# Supplementary Text

## 1 Serostudy analysis details

We used data from a 2013 study *(10)* on the seroprevalence of IgG and IgM antibodies against the Spike (S) protein of the four endemic HCoV strains in a cross-section of the population in Beijing, none of whom exhibited symptoms. A striking feature of these data is that IgM titers are undetectable in all of the more than 140 subjects ages 15 yr and older. This observation combined with general knowledge of the the IgM response *(36)* suggests that S-specific IgM is only elicited during primary infection. Additionally, IgM titers decay quickly, which makes IgM seropositivity a useful marker of recent primary infection.

Although there are a number of studies that analyze the seroprevalence of antibody titers against endemic HCoV's (see *(37)* for a summary of these data), we chose the Zhou study in particular because they (1) measure IgM and IgG separately, (2) analyze all four endemic HCoVs with the same methodology, (3) have multiple sampling ages during childhood, allowing the data to capture the rise in seroprevalence of both IgG and IgM within the first ten or so years of life, and (4) have adult time points that show sustained IgG titers but the absence of IgM. We highlight that we use these antibody data as markers of infection to estimate transmission rates and the force of infection; we do not assume their presence provides protective immunity. (Some of the other studies assess neutralizing antibodies in particular, which are a less sensitive marker of infection, although they may be more strongly correlated with protective immunity.)

We calculate error bars on the seroprevalence for both IgM and IgG for each of the four strains. We assume the data for both IgM and IgG stem from a binomial process where the probability of seropositivity in age group $j$ is $p_j$, estimated by $\hat{p_j}$ and the sample size for each age group is $N_j$. The 95% confidence interval around the mean proportion seropositive for each age group is then

$$1.96\sqrt{\frac{\hat{p_j}(1-\hat{p_j})}{N_j}} \tag{1}$$

We further estimate the MAPI following the simple catalytic model framework *(38)* using only the IgM data to identify the distribution of age at attack. We assume that the cases are uniformly distributed within each age group – a more accurate estimate could be obtained from the raw data with smaller age bins; unfortunately we were unable to gain access to it. For each HCoV strain, $s$, we create a vector, $A_s$ with length $L$ containing the ages of IgM seropositivity (using the midpoints of each age range). We assume this is a reasonable reflection of ages of first infection, as IgM titers increase only during primary infection and decay in a matter of weeks *(39)*. This analysis assumes that infections are at a steady state and the age distribution of recent cases (IgM positive individuals) in this cross section of the population is therefore represents the distribution of ages at which

individuals first get infected. The 95% CI for the MAPI for each strain, $s$, is then estimated by

$$\text{MAPI}_s = \frac{1}{L}\sum A_s \pm 1.96\sqrt{\frac{\text{Var}(A_s)}{L}} \tag{2}$$

## 2 Model derivation

We derived the model presented in SI Fig 1 by combining three key sources of information: (1) classic SIRS disease transmission models, (2) separated functional immune efficacies (IE's, *(7)*), and (3) a human reinfection experiment with HCoV 229e in fifteen healthy adult volunteers *(8)*.

In the aforementioned reinfection experiment, all subjects had serum specific antibodies at the start, suggesting that participants had already experienced a primary infection. The first experimental exposure resulted in viral replication and a boosting of IgG titers in ten of the fifteen participants; the group that supported viral replication had lower serum specific IgG, IgA and nasal IgA levels prior to exposure and shed virus for on average 5.6 days; eight out of ten had cold symptoms. Antibody titers increased significantly approximately a week after infection and then slowly decayed over the course of the next year. Among the five participants who did not get infected following exposure at the beginning of the trial, antibody titers remained relatively constant following exposure; however their IgG titers did drop significantly by the end of the year.

One year after the initial exposure, fourteen of the fifteen participants were re-exposed. All five who had not sustained an infection the first time became infected (their $IE_S$ waned) and one developed cold symptoms ($IE_P$ was still strong for four of the five). Six of the nine who had supported viral replication a year earlier sustained an infection following exposure the second time (their $IE_S$ waned within the span of year) but none developed cold symptoms (they retained $IE_P$); the other three did not become infected following exposure. Among all who got infected at the second time point, the mean duration of viral shedding was only 2.0 days, suggesting that $IE_I$ had not waned completely.

Based on these observations, the following are the basic equations that correspond to SI Fig 1.

$$\frac{dS}{dt} = \mu N - \beta S(I_1 + \rho I_2) - \mu S \tag{3}$$
$$\frac{dI_1}{dt} = \beta S(I_1 + \rho I_2) - (\gamma + \mu) I_1 \tag{4}$$
$$\frac{dR_1}{dt} = \gamma(I_1 + I_2) - (\mu + \omega) R_1 \tag{5}$$
$$\frac{dR_2}{dt} = \omega R_1 - \beta R_2(I_1 + \rho I_2) - \mu R_2 \tag{6}$$
$$\frac{dI_2}{dt} = \beta R_2(I_1 + \rho I_2) - (\gamma + \mu) I_2 \tag{7}$$

where $\mu$ is the birth and death rate, set at 0.02/yr for the steady state simulations. All other parameters and ranges used are described in main text Table 1.

## 2.1 Steady-state analysis

The above equations are used for steady state analysis of the predicted mean ages of primary infection (MAPIs, Fig 2B). The model-predicted MAPI for a given set of parameters is calculated as the waiting time from birth to first infection according to the following equation:

$$\text{MAPI} = \frac{1}{\beta \hat{I_1} + \rho \beta \hat{I_2}} \text{ yr} \tag{8}$$

where $\hat{I}_i$ is the equilibrium proportion of the population in class $I_i$.

The equilibrium values are calculated by first running a short (100 iterations = 1/10 yr) numerical simulation using a wrapper for the R function `lsoda` and then using the final values as estimates to start the Newton-Raphson method to find equilibria as implemented in the R package `rootSolve`, function `stode`.

We additionally calculate the proportion of cases caused by reinfections as follows:

$$\frac{\rho \hat{I_2}}{\hat{I_1} + \rho \hat{I_2}} \tag{9}$$

In addition to the results shown in the main text for $R_0 = 5$, we here show figures parallel to Fig 2b for $R_0 = 2$ and $R_0 = 10$ (SI Fig 2).

## 2.2 Transient to endemic dynamic simulations

To incorporate seasonality with a peak in early January (modeling on influenza and seasonal coronaviruses) and the introduction of the virus in early March (as was approximately observed with CoV-2 in the US), cases are introduced at t=0 and we allow $\beta$ to fluctuate annually according to

$$\beta = \beta_0[1 + \beta_1 \cos(2\pi t + \frac{\pi}{3})] \tag{10}$$

where $\beta_0$ is the mean value of $\beta$, and $\beta_1$ is the amplitude of the sin wave. All results shown here use $\beta_1 = 0.2$ (SI Figs 4-11 and Figs 2 & 3 in the main text).

Additionally, to incorporate the age-specific infection fatality ratios, death rates ($\delta$), and the current age distribution of the US population, we separate each immune state, $X$, into nine age classes $X_j$ with 10-yr widths for the first eight classes. The aging rates correspond to the width of the age classes; the death rates and age distribution are taken from US data. This yields the following equations:

$$\frac{dS_j}{dt} = \mu N + \lambda_j S_j - \beta S_j \sum_{j=1}^{J} (I_{1j} + \rho I_{2j}) - (\delta_j + \lambda_{j+1}) S_j \tag{11}$$

$$\frac{dI_{1j}}{dt} = \lambda_j I_1 + \beta S_j \sum_{j=1}^{J} (I_{1j} + \rho I_{2j}) - (\gamma + \delta_j + \lambda_{j+1}) I_{1j} \tag{12}$$

$$\frac{dR_{1j}}{dt} = \lambda_j R_{1j} + \gamma(I_{1j} + I_{2j}) - (\delta_j + \omega + \lambda_{j+1}) R_{1j} \tag{13}$$

$$\frac{dR_{2j}}{dt} = \lambda_j R_{2j} + \omega R_{1j} - \beta R_{2j} \sum_{j=1}^{J} (I_{1j} + \rho I_{2j}) - (\delta_j + \lambda_{j+1}) R_2 \tag{14}$$

$$\frac{dI_{2j}}{dt} = \lambda_j I_{2j} + \beta R_{2j} \sum_{j=1}^{J} (I_{1j} + \rho I_{2j}) - (\gamma + \delta_j) I_{2j} \tag{15}$$

where $N(t) = \sum_{j=1}^{J} X_t$ is the total population size at time $t$. The birth rate, $\mu$, is a vector of length nine, containing the overall population birthrate (based on demographic data) followed by zeros for all subsequent age classes (i.e., people are only born into the youngest age class). The age-specific death rates, $\delta_j$, are fixed at values estimated from demographic data. The aging rates, $\lambda_j$, are contained in a vector of length ten: $(0, 0.1, 0.1, 0.1, 0.1, 0.1, 0.1, 0.1, 0.04, 0)$. We fix $\gamma$ at $\frac{365}{9}$ corresponding to an infectious period that lasts on average nine days. $\beta_0$ is calculated according to $\beta_0 = R_0(\gamma + \mu)$. We consider a range of values of $R_0$ (2-10), $\omega$ (0-2), and $\rho$ (0-1).

The age-specific death rates were inferred from CDC data Health Statistics *(40)*, and were calculated as follows:

```
death_rate_age<-as.data.frame(cbind(age=seq(25,95,by=10),
    number=c(30154,58844,80380,164837,374836,543778,675205,880280),
    rate=c(70.2,128.8,194.7,395.9,886.7,1783.3,4386.1,13450.7)/100000))
```

```
death_rate.glm<-with(
    death_rate_age,glm(rate ~ age,
        family=gaussian(link='log'))
    )

pred.ages<-seq(5,85,length=9)
pred_death_rate<-exp(predict(death_rate.glm, data.frame(age=seq(0,100,by=0.5))))
mod.pred<-round(exp(predict(death_rate.glm, data.frame(age=pred.ages))),5)
print(mod.pred)
```

```
##       1       2       3       4       5       6       7       8       9
## 0.00001 0.00003 0.00008 0.00024 0.00068 0.00197 0.00565 0.01623 0.04662
```

The ages used in the model prediction for death rates were the midpoints of the age classes (e.g. 5, 15, 25yr, etc). We used the death rate for 85 yr olds as the highest death rate.

The initial conditions were set so the population was distributed into the nine susceptible classes according to the age distribution of the US population *(41)*.

One infected individuals was seeded into each age group's $I_1$ class.

### 2.3 Calculating infections and the infection fatality rate from simulations

The following steps were used to calculate the number of daily infections and 6-month moving average infection fatality rate (IFR):

1. Numerically integrate equations with chosen parameters and initial conditions as described above using the R function `lsoda` with a time step of one day (1/365 yr).

2. Calculate the probability of staying in $I_1$ for a timestep of one day given that you're already there.
   In the simplest version of the model we consider here, this can be calculated using the cumulative distribution function, $F$:

$$P(\text{stay in I in time step}\Delta t) = 1 - F(\gamma, \Delta t) \tag{16}$$

```
gamma=365/9
time.step=1/365
prob.stay=1-pexp(rate=gamma, time.step)
print(prob.stay)
```

```
## [1] 0.8948393
```

3. For each age group, calculate the number of new primary infections in each time step, $X_t$

$$I_{t1} = I_{t0}P(\text{stay in I in time step}) + X_t \tag{17}$$
$$X_t = I_{t1} - I_{t0}P(\text{stay in I in time step}) \tag{18}$$

```
I_t1 <- tail(out[, 'I1'],-1)
I_t0 <- head(out[, 'I1'],-1)
X = I_t1 - I_t0 * prob.stay
```

4. Calculate the projected number of HCoV-induced deaths in each age group based on the age-specific IFRs.

$$\text{deaths}_j = X_j * \text{IFR}_j \tag{19}$$

5. For every 6-month window, calculate the overall IFR beginning six months into the pandemic

$$\frac{\sum_{j=1}^{J} \text{deaths}_j}{\sum_{j=1}^{J} X_j} \tag{20}$$

The key result that the overall IFR drops to something akin to seasonal influenza (0.001), is robust across a wide range of values for $R_0$, $\omega$ and $\rho$ for COVID-like IFRs.

# 3 Model extensions: Gamma-distributed durations of immunity & gradual build-up of immunity

The central results are robust to a model formulation that incorporates a more biologically realistic distribution of how long individuals retain sterilizing immunity (remain in class $R_{1B}$ and the possibility that protective immunity is acquired over the course of the first two infections ($I_{1A}$ and $I_{1B}$) rather than immediately following primary infection. We assume that individuals who have recovered from a primary infection ($R_{1A}$) and do not yet have protective immunity can become infected ($I_{1B}$) and are then susceptible to death at the same rate as $I_{1A}$ while transmitting only as much as $I_2$. The force of infection is therefore calculated according to

$\Lambda = \beta S_j \sum_{j=1}^{J} (I_{1Aj} + \rho(I_{1Bj} + I_{2j}))$.

The Gamma-distributed duration of sterilizing immunity ($R_{1B}$) is modeled by a chain of $\Gamma$ $R_{1B}$ compartments.

We additionally incorporate the possibility of immunization at rate $\nu$.

This model is simulated from the following equations:

$$\frac{dS_j}{dt} = \mu N + \lambda_j S_j - \Lambda S_j - (\nu + \delta_j + \lambda_{j+1}) S_j \tag{21}$$

$$\frac{dI_{1Aj}}{dt} = \lambda_j I_{1Aj} + \Lambda S_j - (\gamma + \delta_j + \lambda_{j+1}) I_{1Aj} \tag{22}$$

$$\frac{dR_{1Aj}}{dt} = \lambda_j R_{1Aj} + \gamma I_{1j} - (\delta_j + \nu + \lambda_{j+1}) R_{1Aj} \tag{23}$$

$$\frac{dI_{1Bj}}{dt} = \lambda_j I_{1B} + \Lambda R_{1Aj} - (\gamma + \delta_j + \lambda_{j+1}) I_{1Bj} \tag{24}$$

$$\frac{dR_{1Bj1}}{dt} = \lambda_j R_{1Bj1} + \gamma (I_{1Bj} + I_{2j}) + \nu (S_j + R_{1Aj} + R_{2j}) - (\delta_j + \omega\Gamma + \lambda_{j+1}) R_{1Bj1} \tag{25}$$

$$\frac{dR_{1Bjk}}{dt} = \lambda_j R_{1Bjk} + \omega\Gamma R_{1Bk-1} - (\delta_j + \omega\Gamma + \lambda_{j+1}) R_{1Bjk} \tag{26}$$

$$\frac{dR_{2j}}{dt} = \lambda_j R_{2j} + \omega\Gamma R_{1j\Gamma} - \Lambda R_{2j} - (\delta_j + \lambda_{j+1} + \nu) R_{2j} \tag{27}$$

$$\frac{dI_{2j}}{dt} = \lambda_j I_{2j} + \Lambda R_{2j} - (\gamma + \delta_j) I_{2j} \tag{28}$$

where $k \in (2, \Gamma)$.

The incorporation of Gamma-distributed waning times (using a shape parameter $\Gamma = 10$) helps reconcile the short mean duration of immunity with the observation that in the first nine months of the pandemic reinfections appear to be rare. The smaller variance in durations of immunity additionally contribute to stronger cyclical dynamics in general, amplifying the seasonality (SI Fig 5).

Here, we consider the possibility that it may take two infections to develop fully protective immunity and show that it extends the time it takes to reach a very low overall IFR, but it still happens in on the order of years to a couple decades (SI Figs 6 & 7, compare with Fig 2 in the main text).

Incorporating Gamma-distributed waning times extends this slightly further and makes the transitions more sudden since cases are more highly aggregated in time (SI Figs 8 & 9)

## 4 Social distancing and vaccination

Additionally, we see that keeping $R_0$ below a threshold value (in these simulations approximately 2, e.g., by social distancing and the use of Personal Protective Equipment) allows us to stop the majority of deaths from happening early on, buying time for the development of an effective vaccine and/or treatment (SI Fig 10).

These very low values of $R_0$, which roughly correspond to COVID-19 death rates observed through summer 2020 due to strong social distancing measures, are able to delay the vast majority of infections and deaths, allowing time for the development and roll-out of a vaccine campaign.

We show the utility of a vaccine once contact patterns are allowed to return to normal, here modeled with $R_0 = 4$ (SI Fig 11). We model vaccination as a transition from $S$, $R_{1A}$ or $R_2$ directly to the fully immune class, $R_{1B}$ without experiencing infection and therefore neither risking death nor contributing to the force of infection. Here, we show results for $\nu = 0.51$ which corresponds to an annual vaccine coverage of 40% of the population, akin to the seasonal influenza vaccine uptake. For COVID, a safe and effective vaccine is predicted to save hundreds of thousands of lives in the first year, but continued mass vaccination has very little beneficial effect. Targeted vaccination in subpopulations who are at increased risk and may have reduced capacity to effectively respond to the vaccine may of course still be useful. This type of targeted vaccination could also reduce HCoV-induced deaths from endemic strains, e.g., among immune senescent populations in nursing homes *(42)*. In contrast, were a MERS-like HCoV to emerge, long term mass vaccination at a rate similar to flu vaccine uptake would continue to save hundreds of thousands of lives.

## 5 Loss of immunity kernel

We estimate the duration of sterilizing immunity based on Callow et al. *(8)*, in which six out of nine people who got infected at the start of the experiment were susceptible to reinfection one year later. We can calculate the mean of $\omega$ given this for exponentially distributed waning times setting the CDF equal to 2/3 (SI Fig 12).

$$\frac{1}{\bar{\omega}} = \frac{1}{\log 2/3} = 0.91 \tag{29}$$

```
lambdas=seq(0,2,by=0.01)
plot(lambdas, pexp(1,rate=lambdas), type='l')
abline(h=0.66667, v=1.099)
```

Given this, the estimate for $\omega$ is 1.099 and the mean waiting time is $1/\omega = 0.91$ yr.

We can also find the average duration of immunity for normally distributed waning times (SI Fig 13). We assume that the variance is the same as for the exponential model, $\frac{1}{\lambda^2}$ and the standard deviation is $\frac{1}{\lambda}$.

```
means = seq(0,2,by=0.01)
plot(means,pnorm(1, mean=means, sd=1/1.099), type='l')
abline(h=0.6667)
abline(v=0.61)
```

Here, we find the estimate for the mean of $\omega$ to be 0.61/yr, so the mean waiting time is $\frac{1}{0.61} = 1.64yr$.

## 6 Age-severity curves

We use Verity et al's estimate of the IFR for CoV-2 *(34)*. We estimate the age-severity curves for CoV-1 and MERS using published data (SARS CoV-1 *(33)*, and MERS *(5)*). We fit a generalized linear model to each data set to estimate a smoothed IFR as a function of age. We use a binomial model in which total cases in an age group is considered the number of trials, and the number of deaths is considered the number of 'successes'. For MERS, we allow the function to be a third degree polynomial to account for the non-monotonicity of the data. We consider a second degree polynomial for SARS CoV-1, since the relationship between age and IFR appears monotonic in the data for these. Our code is included below.

# Supplementary Figures

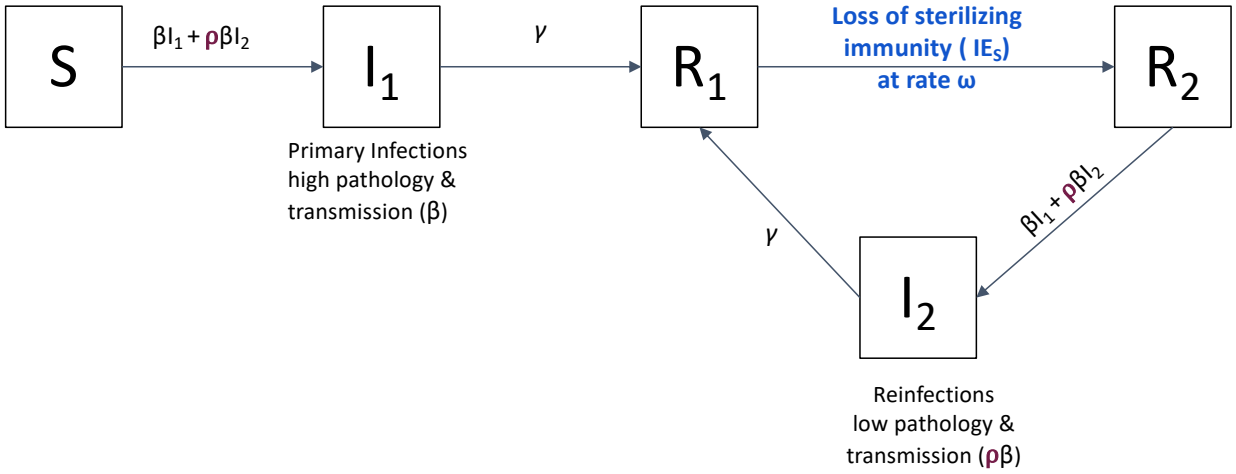


Fig. S1. Compartmental model for HCoV epidemiology, incorporating the following features of natural HCoV infections: recovered individuals ($R_1$) have sterilizing immunity (high $IE_S$) which wanes at rate $\omega$; individuals whose sterilizing immunity has waned ($R_2$) can become reinfected ($I_2$), albeit with mild symptoms ($IE_P$ is high) and reduced transmission to others (compared with transmission from primary infections, i.e., $\rho \leq 1$). We use an age-structured version of this model with parameters for demography of the US population in our simulations of transient dynamics and vaccination. See SI Sec 2 for equations and details.

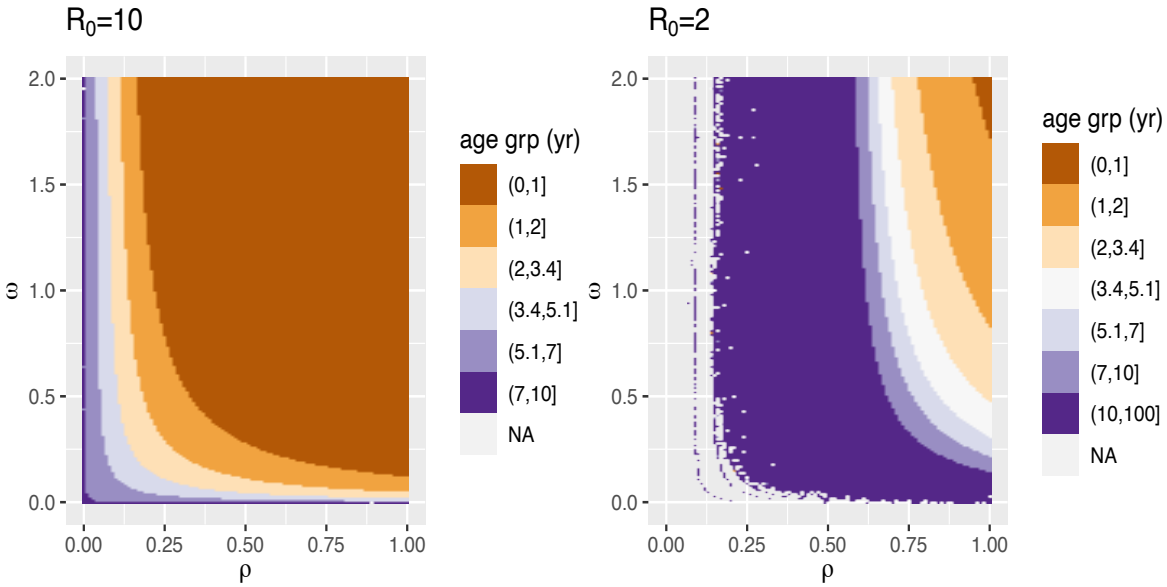


Fig. S2. Mean age of primary infection calculated from the steady state of the model withacross various parameters.

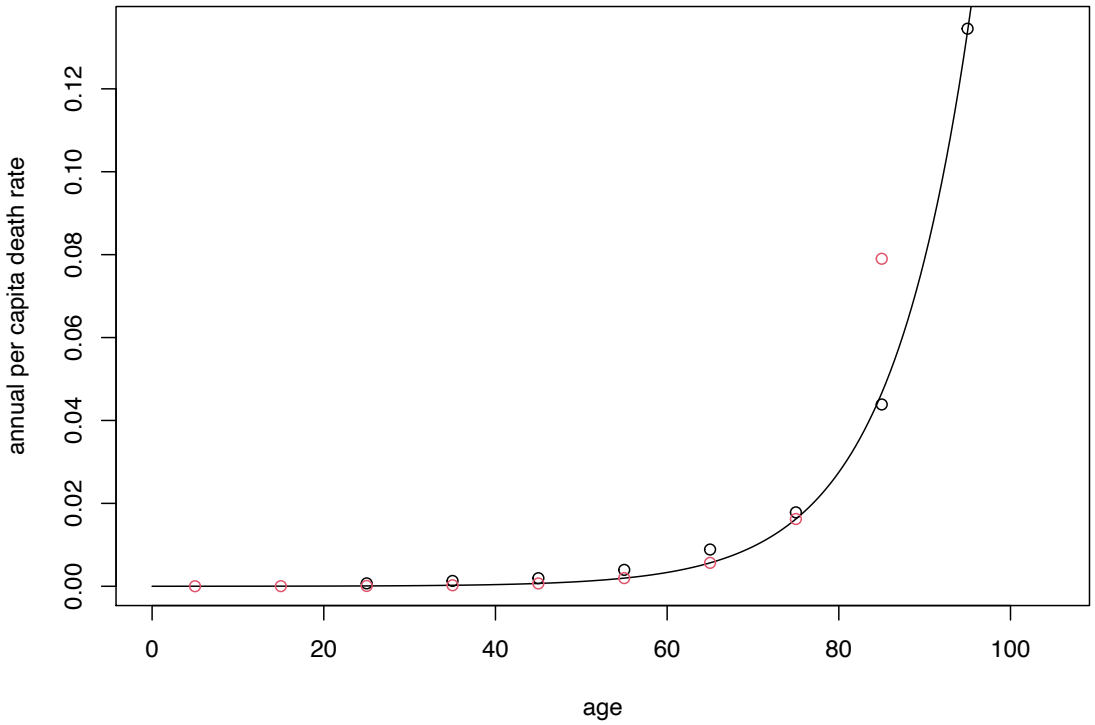


Fig. S3. Age specific death rate in the US. Red points represent data, the black line is the best fit curve and the black points are the predicted values used in simulations.

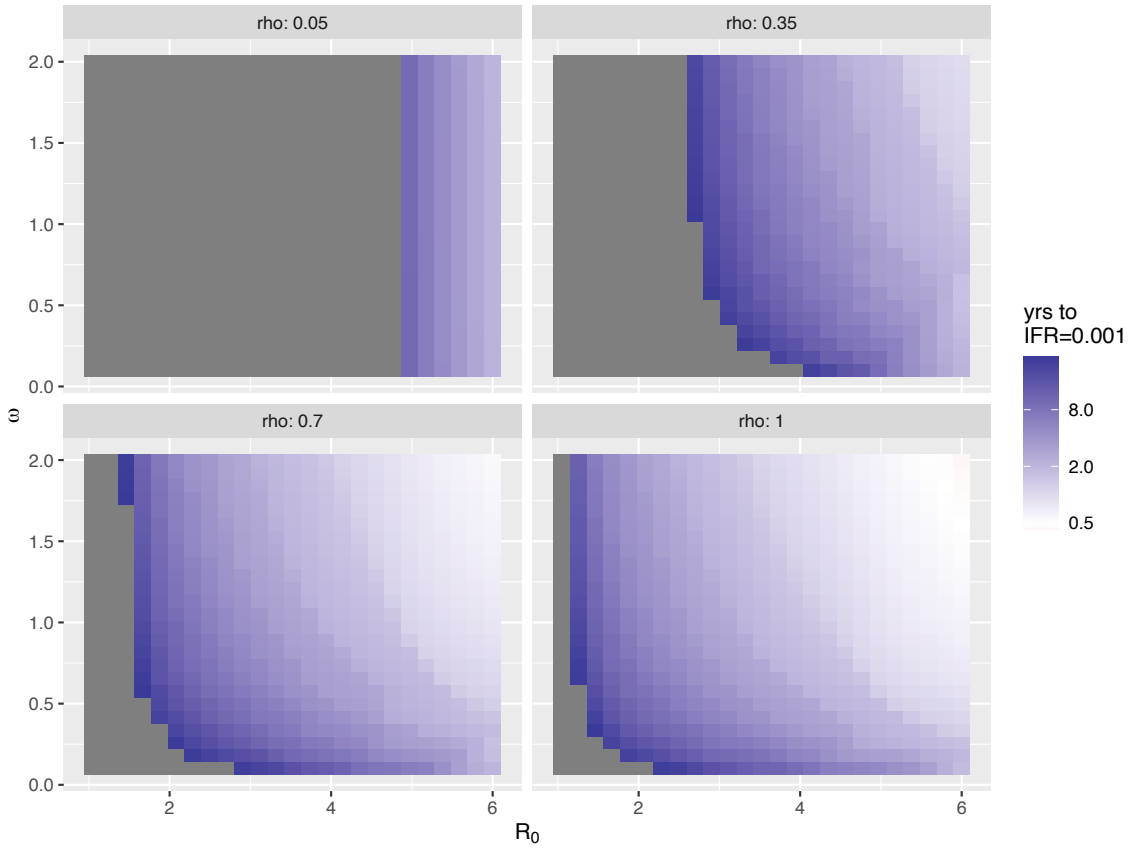


Fig. S4. Time to IFR=0.001, parallel to main text Fig 2b.

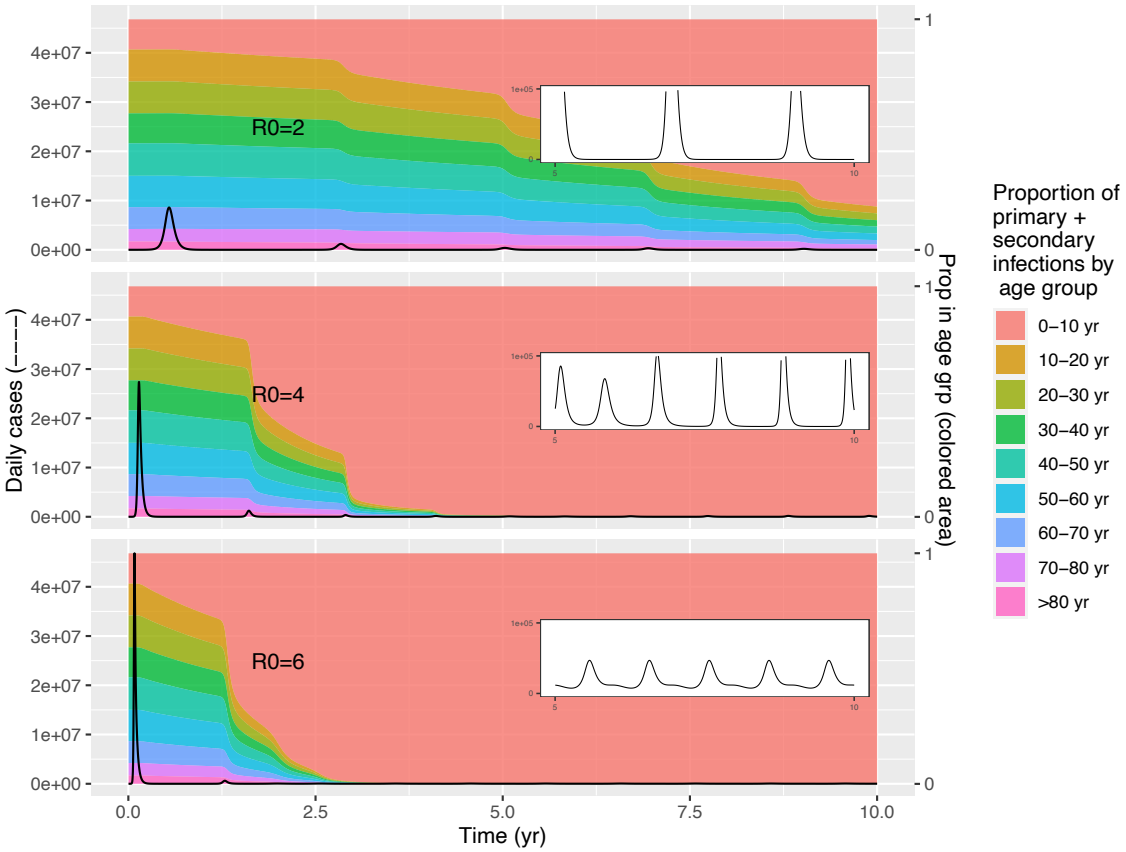


Fig. S5. Projected age distributions of primary + secondary infections with Gamma-distributed sterilizing immunity. $\omega = 1, \rho = 0.7, \nu = 0, \gamma = 365/9, \Gamma = 10$.

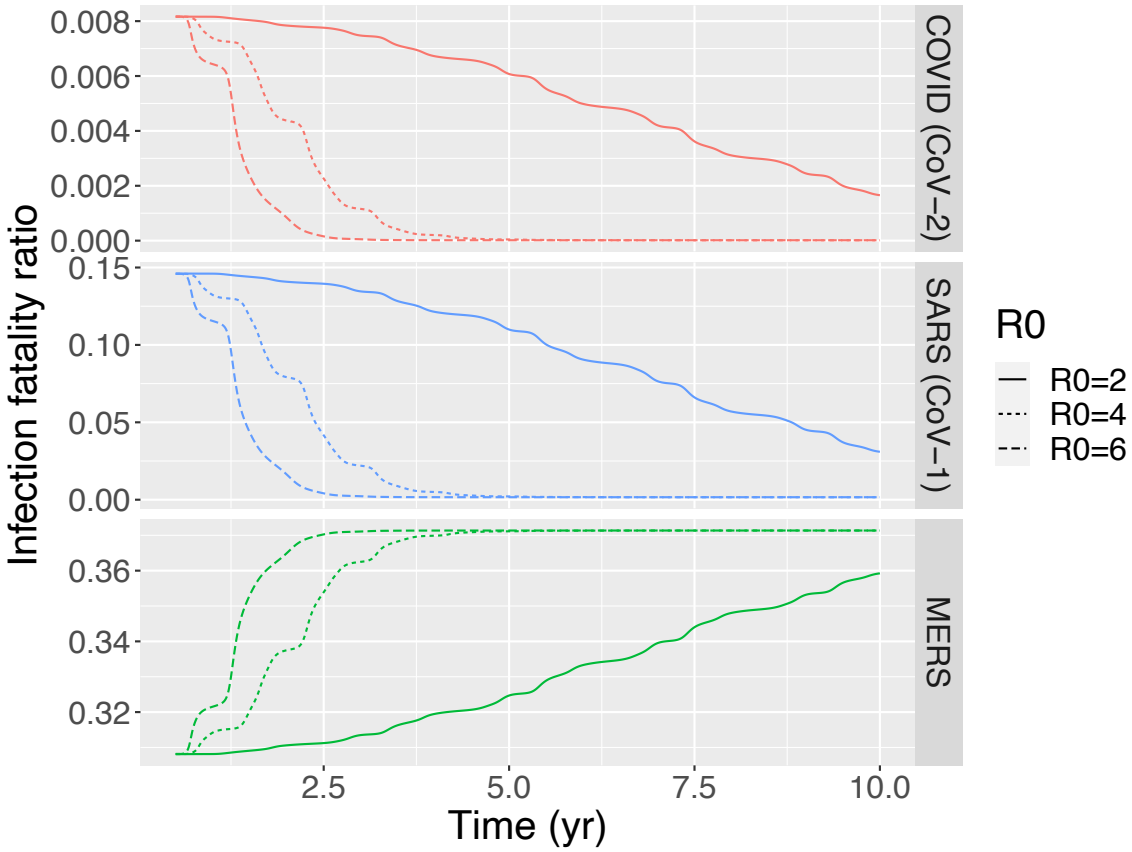


Fig. S6. Projected IFRs; first two infections possibly lead to death. $\omega = 1, \rho = 0.7, \nu = 0, \gamma = 365/9, \Gamma = 1$.

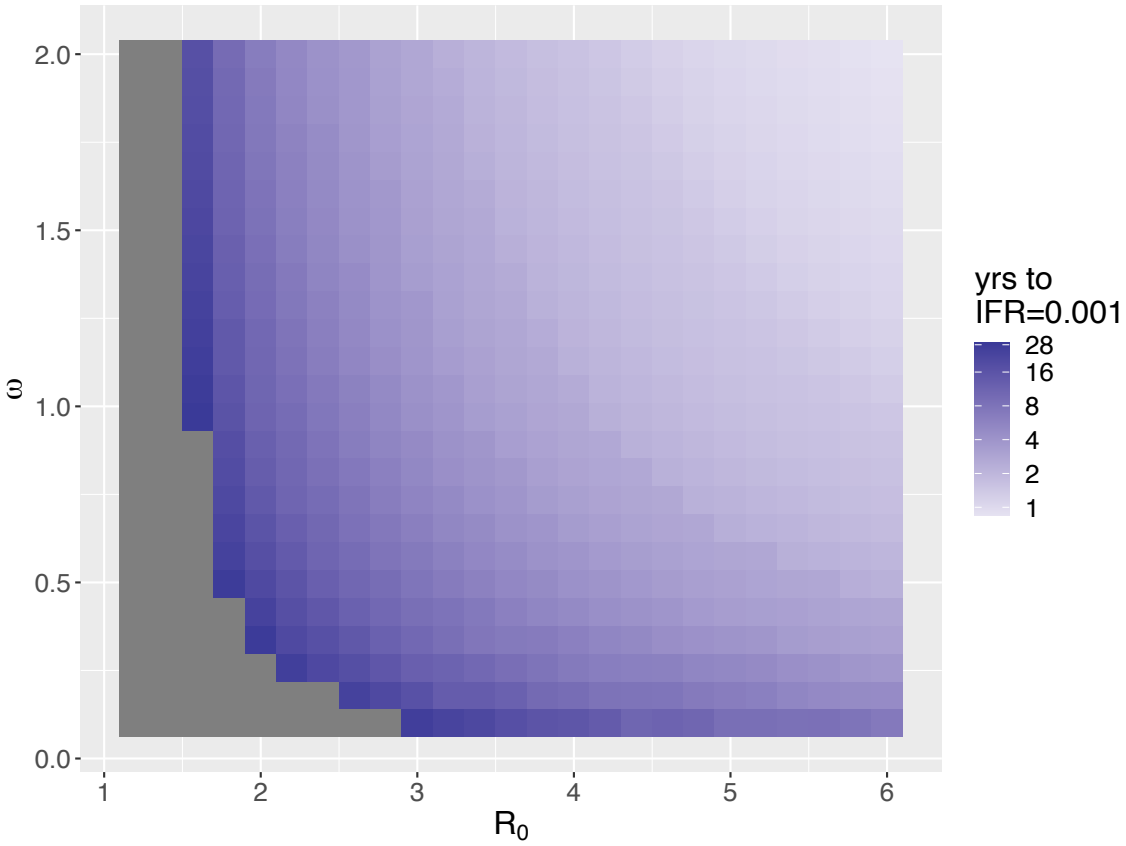


Fig. S7. Time to overall IFR=0.001 where first two infections have a non-zero IFR. $\nu = 0, \gamma = 365/9, \Gamma = 1$.

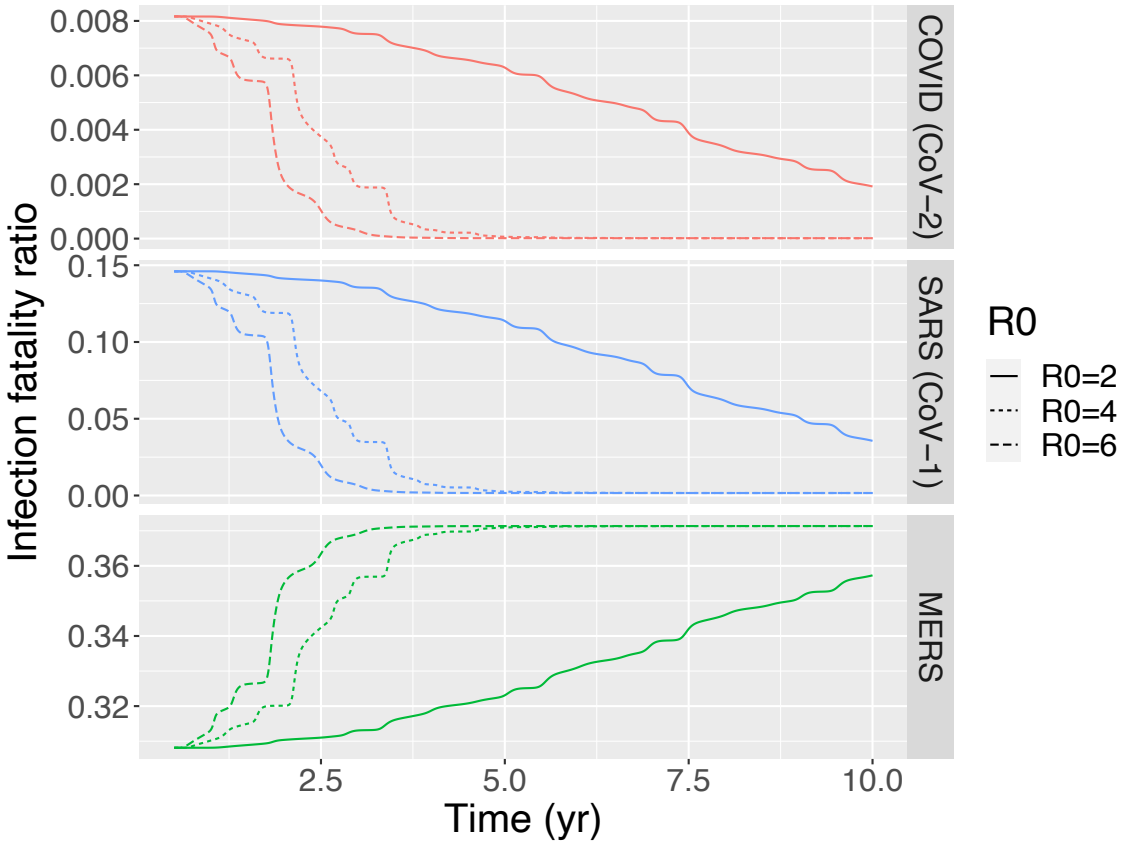


Fig. S8. Projected IFRs with the first two infections possibly leading to death and the duration of sterilizing immunity Gamma distributed with shape parameter 10. $\omega = 1, \rho = 0.7, \nu = 0, \gamma = 365/9, \Gamma = 10$.

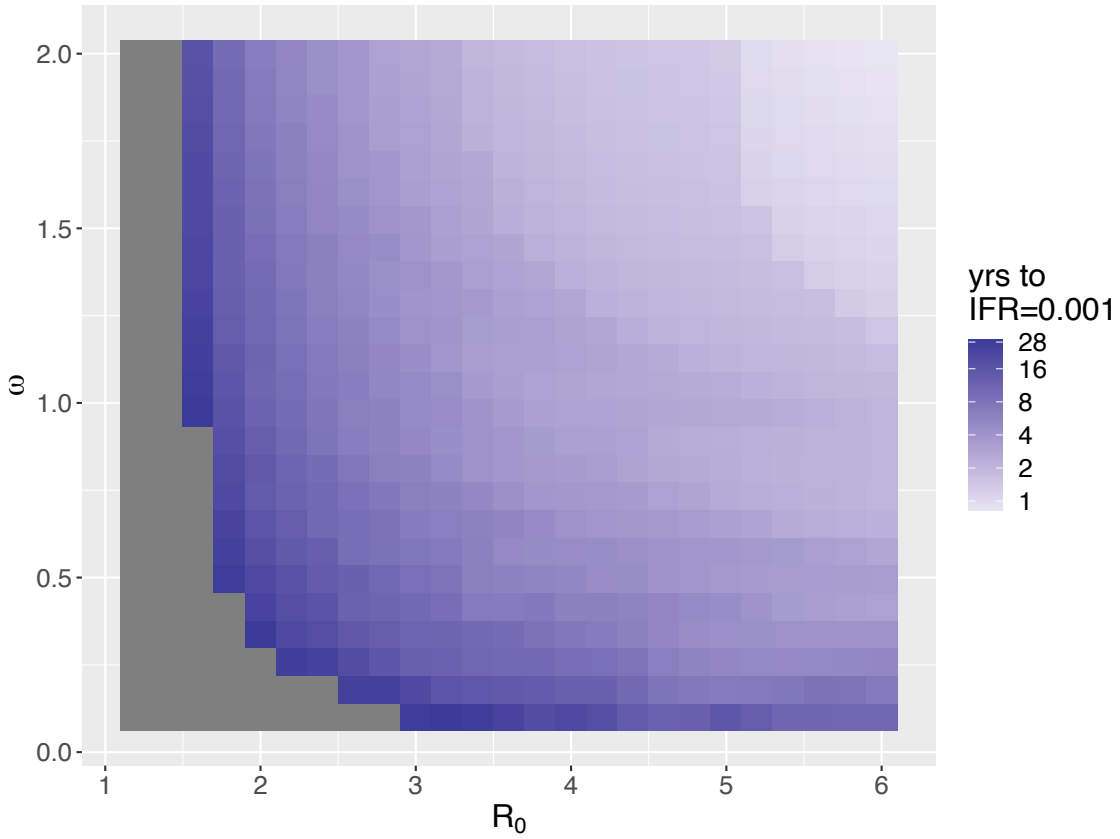


Fig. S9. Time to overall IFR=0.001 with Gamma distributed waning of immunity. $\nu = 0, \gamma = 365/9, \Gamma = 10$.

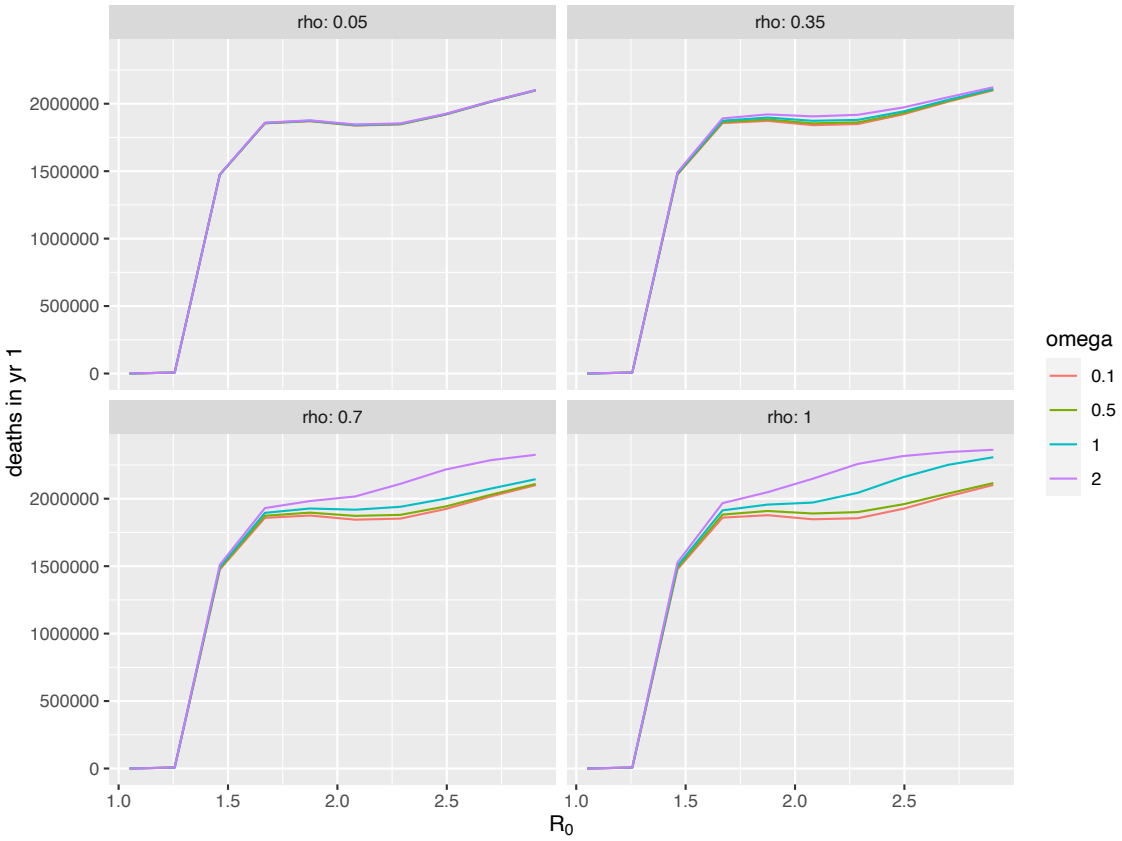


Fig. S10. Number of infection-induced deaths in first year after emergence. When reinfection occurs quickly and is transmissible (high $\omega$ and $\rho$), the total number of infection-induced deaths is close to independent of $R_0$ for $R_0 > 2$.

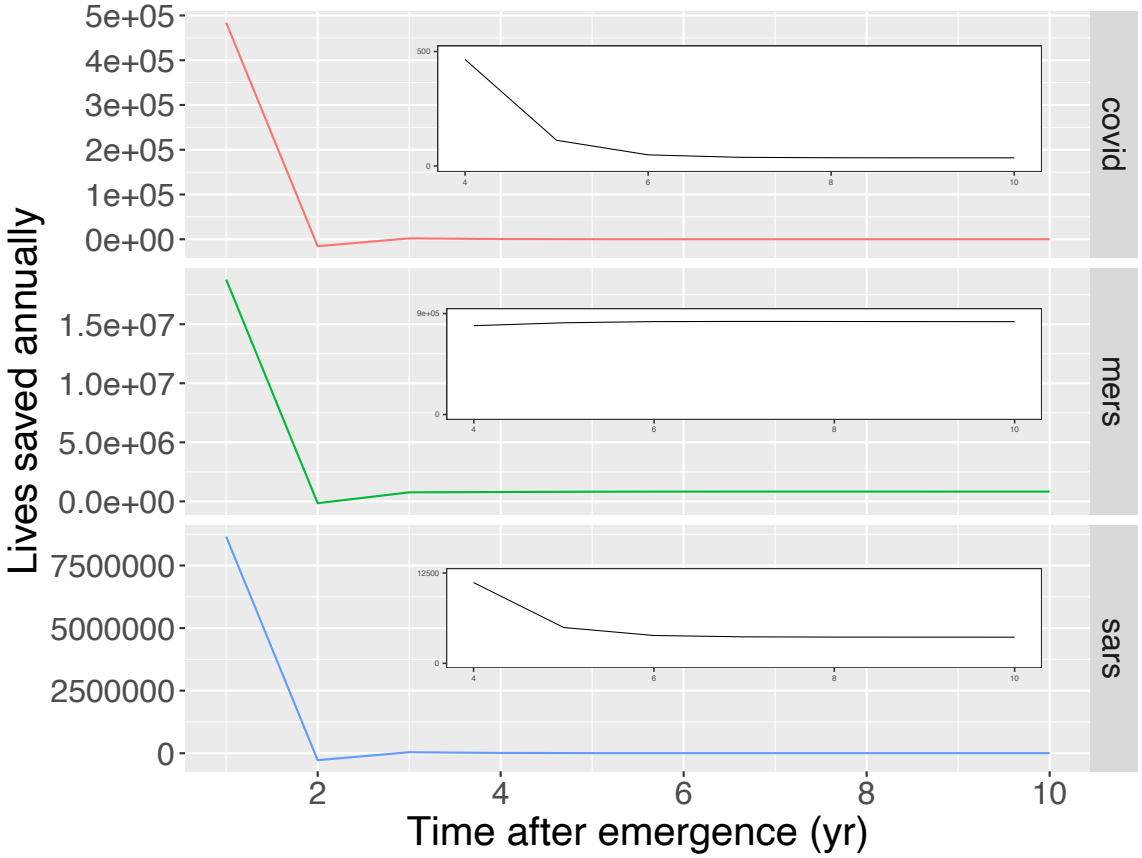


Fig. S11. Difference between projected annual deaths without and with 40% annual vaccine coverage.

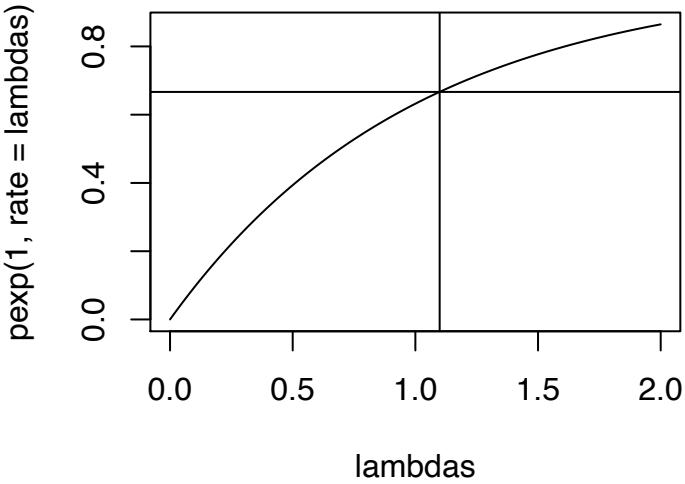


Fig. S12. Estimated duration of immunity given exponentially distributed waning times based on Callow et al.

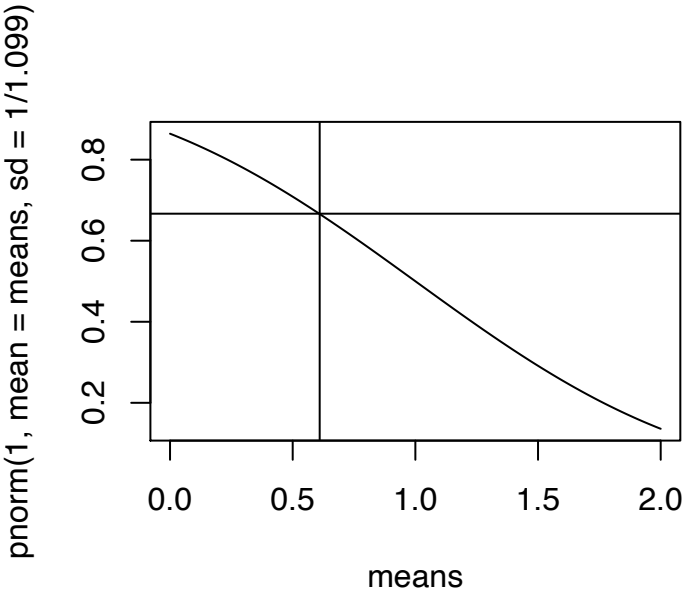


Fig. S13. Estimated duration of immunity given normally distributed waning times based on Callow et al.

**References and Notes**


1. S. Cobey, Modeling infectious disease dynamics. *Science* **368**, 713–714 (2020). doi:10.1126/science.abb5659 Medline

2. H. E. Randolph, L. B. Barreiro, Herd immunity: Understanding COVID-19. *Immunity* **52**, 737–741 (2020). doi:10.1016/j.immuni.2020.04.012 Medline

3. C. Fraser, S. Riley, R. M. Anderson, N. M. Ferguson, Factors that make an infectious disease outbreak controllable. *Proc. Natl. Acad. Sci. U.S.A.* **101**, 6146–6151 (2004). doi:10.1073/pnas.0307506101 Medline

4. S. Su, G. Wong, W. Shi, J. Liu, A. C. K. Lai, J. Zhou, W. Liu, Y. Bi, G. F. Gao, Epidemiology, genetic recombination, and pathogenesis of coronaviruses. *Trends Microbiol.* **24**, 490–502 (2016). doi:10.1016/j.tim.2016.03.003 Medline

5. M. Salamatbakhsh, K. Mobaraki, S. Sadeghimohammadi, J. Ahmadzadeh, The global burden of premature mortality due to the Middle East respiratory syndrome (MERS) using standard expected years of life lost, 2012 to 2019. *BMC Public Health* **19**, 1523 (2019). doi:10.1186/s12889-019-7899-2 Medline

6. S. Ruan, Likelihood of survival of coronavirus disease 2019. *Lancet Infect. Dis.* **20**, 630–631 (2020). doi:10.1016/S1473-3099(20)30257-7 Medline

7. M. E. Halloran, I. M. Longini, C. J. Struchiner, *Design and Analysis of Vaccine Studies* (Statistics for Biology and Health, Springer, 2010).

8. K. A. Callow, H. F. Parry, M. Sergeant, D. A. J. Tyrrell, The time course of the immune response to experimental coronavirus infection of man. *Epidemiol. Infect.* **105**, 435–446 (1990). doi:10.1017/S0950268800048019 Medline

9. A. F. Bradburne, M. L. Bynoe, D. A. Tyrrell, Effects of a “new” human respiratory virus in volunteers. *BMJ* **3**, 767–769 (1967). doi:10.1136/bmj.3.5568.767 Medline

10. W. Zhou, W. Wang, H. Wang, R. Lu, W. Tan, First infection by all four non-severe acute respiratory syndrome human coronaviruses takes place during childhood. *BMC Infect. Dis.* **13**, 433 (2013). doi:10.1186/1471-2334-13-433 Medline

11. M. Galanti, J. Shaman, Direct observation of repeated infections with endemic coronaviruses. *J. Infect. Dis.* jiaa392 (2020). doi:10.1093/infdis/jiaa392 Medline

12. A. W. D. Edridge, J. Kaczorowska, A. C. R. Hoste, M. Bakker, M. Klein, K. Loens, M. F. Jebbink, A. Matser, C. M. Kinsella, P. Rueda, M. Ieven, H. Goossens, M. Prins, P. Sastre, M. Deijs, L. van der Hoek, Seasonal coronavirus protective immunity is short-lasting. *Nat. Med.* **26**, 1691–1693 (2020). doi:10.1038/s41591-020-1083-1 Medline

13. R. Yan, Y. Zhang, Y. Li, L. Xia, Y. Guo, Q. Zhou, Structural basis for the recognition of SARS-CoV-2 by full-length human ACE2. *Science* **367**, 1444–1448 (2020). doi:10.1126/science.abb2762 Medline

14. K. Kuba, Y. Imai, S. Rao, H. Gao, F. Guo, B. Guan, Y. Huan, P. Yang, Y. Zhang, W. Deng, L. Bao, B. Zhang, G. Liu, Z. Wang, M. Chappell, Y. Liu, D. Zheng, A. Leibbrandt, T. Wada, A. S. Slutsky, D. Liu, C. Qin, C. Jiang, J. M. Penninger, A crucial role of

angiotensin converting enzyme 2 (ACE2) in SARS coronavirus-induced lung injury. *Nat. Med.* **11**, 875–879 (2005). doi:10.1038/nm1267 Medline

15. Y. Imai, K. Kuba, S. Rao, Y. Huan, F. Guo, B. Guan, P. Yang, R. Sarao, T. Wada, H. Leong-Poi, M. A. Crackower, A. Fukamizu, C.-C. Hui, L. Hein, S. Uhlig, A. S. Slutsky, C. Jiang, J. M. Penninger, Angiotensin-converting enzyme 2 protects from severe acute lung failure. *Nature* **436**, 112–116 (2005). doi:10.1038/nature03712 Medline

16. T. S. Fung, D. X. Liu, Human coronavirus: Host-pathogen interaction. *Annu. Rev. Microbiol.* **73**, 529–557 (2019). doi:10.1146/annurev-micro-020518-115759 Medline

17. S. P. Weisberg, T. J. Connors, Y. Zhu, M. R. Baldwin, W.-H. Lin, S. Wontakal, P. A. Szabo, S. B. Wells, P. Dogra, J. Gray, E. Idzikowski, D. Stelitano, F. T. Bovier, J. Davis-Porada, R. Matsumoto, M. M. L. Poon, M. Chait, C. Mathieu, B. Horvat, D. Decimo, K. E. Hudson, F. D. Zotti, Z. C. Bitan, F. La Carpia, S. A. Ferrara, E. Mace, J. Milner, A. Moscona, E. Hod, M. Porotto, D. L. Farber, Distinct antibody responses to SARS-CoV-2 in children and adults across the COVID-19 clinical spectrum. *Nat. Immunol.* **22**, 25–31 (2021). doi:10.1038/s41590-020-00826-9 Medline

18. A. Antia, H. Ahmed, A. Handel, N. E. Carlson, I. J. Amanna, R. Antia, M. Slifka, Heterogeneity and longevity of antibody memory to viruses and vaccines. *PLOS Biol.* **16**, e2006601 (2018). doi:10.1371/journal.pbio.2006601 Medline

19. F. Tang, Y. Quan, Z.-T. Xin, J. Wrammert, M.-J. Ma, H. Lv, T.-B. Wang, H. Yang, J. H. Richardus, W. Liu, W.-C. Cao, Lack of peripheral memory B cell responses in recovered patients with severe acute respiratory syndrome: A six-year follow-up study. *J. Immunol.* **186**, 7264–7268 (2011). doi:10.4049/jimmunol.0903490 Medline

20. N. Le Bert, A. T. Tan, K. Kunasegaran, C. Y. L. Tham, M. Hafezi, A. Chia, M. H. Y. Chng, M. Lin, N. Tan, M. Linster, W. N. Chia, M. I.-C. Chen, L.-F. Wang, E. E. Ooi, S. Kalimuddin, P. A. Tambyah, J. G.-H. Low, Y.-J. Tan, A. Bertoletti, SARS-CoV-2-specific T cell immunity in cases of COVID-19 and SARS, and uninfected controls. *Nature* **584**, 457–462 (2020). doi:10.1038/s41586-020-2550-z Medline

21. R. Channappanavar, C. Fett, J. Zhao, D. K. Meyerholz, S. Perlman, Virus-specific memory CD8 T cells provide substantial protection from lethal severe acute respiratory syndrome coronavirus infection. *J. Virol.* **88**, 11034–11044 (2014). doi:10.1128/JVI.01505-14 Medline

22. R. Eguia, K. H. D. Crawford, T. Stevens-Ayers, L. Kelnhofer-Millevolte, A. L. Greninger, J. A. Englund, M. J. Boeckh, J. D. Bloom, A human coronavirus evolves antigenically to escape antibody immunity. bioRxiv 2020.12.17.423313 [Preprint]. 18 December 2020. https://doi.org/10.1101/2020.12.17.423313.

23. M. Voysey, S. A. C. Clemens, S. A. Madhi, L. Y. Weckx, P. M. Folegatti, P. K. Aley, B. Angus, V. L. Baillie, S. L. Barnabas, Q. E. Bhorat, S. Bibi, C. Briner, P. Cicconi, A. M. Collins, R. Colin-Jones, C. L. Cutland, T. C. Darton, K. Dheda, C. J. A. Duncan, K. R. W. Emary, K. J. Ewer, L. Fairlie, S. N. Faust, S. Feng, D. M. Ferreira, A. Finn, A. L. Goodman, C. M. Green, C. A. Green, P. T. Heath, C. Hill, H. Hill, I. Hirsch, S. H. C. Hodgson, A. Izu, S. Jackson, D. Jenkin, C. C. D. Joe, S. Kerridge, A. Koen, G. Kwatra, R. Lazarus, A. M. Lawrie, A. Lelliott, V. Libri, P. J. Lillie, R. Mallory, A. V. A. Mendes, E. P. Milan, A. M. Minassian, A. McGregor, H. Morrison, Y. F. Mujadidi, A. Nana, P. J.

O'Reilly, S. D. Padayachee, A. Pittella, E. Plested, K. M. Pollock, M. N. Ramasamy, S. Rhead, A. V. Schwarzbold, N. Singh, A. Smith, R. Song, M. D. Snape, E. Sprinz, R. K. Sutherland, R. Tarrant, E. C. Thomson, M. E. Török, M. Toshner, D. P. J. Turner, J. Vekemans, T. L. Villafana, M. E. E. Watson, C. J. Williams, A. D. Douglas, A. V. S. Hill, T. Lambe, S. C. Gilbert, A. J. Pollard; Oxford COVID Vaccine Trial Group, Safety and efficacy of the ChAdOx1 nCoV-19 vaccine (AZD1222) against SARS-CoV-2: An interim analysis of four randomised controlled trials in Brazil, South Africa, and the UK. *Lancet* S0140-6736(20)32661-1 (2020). doi:10.1016/S0140-6736(20)32661-1 Medline

24. European Centre for Disease Prevention and Control, "Reinfection with SARS-CoV: Considerations for public health response" (ECDC, 2020); www.ecdc.europa.eu/sites/default/files/documents/Re-infection-and-viral-shedding-threat-assessment-brief.pdf.

25. L. J. Abu-Raddad, H. Chemaitelly, J. A. Malek, A. A. Ahmed, Y. A. Mohamoud, S. Younuskunju, H. H. Ayoub, Z. Al Kanaani, A. Al Khal, E. Al Kuwari, A. A. Butt, P. Coyle, A. Jeremijenko, A. H. Kaleeckal, A. N. Latif, R. M. Shaik, H. F. A. Rahim, H. M. Yassine, M. G. Al Kuwari, H. E. Al Romaihi, M. H. Al-Thani, R. Bertollini, Assessment of the risk of SARS-CoV-2 reinfection in an intense re-exposure setting. *Clin. Infect. Dis.* 10.1093/cid/ciaa1846 (2020). doi:10.1093/cid/ciaa1846 Medline

26. J. S. Weitz, S. J. Beckett, A. R. Coenen, D. Demory, M. Dominguez-Mirazo, J. Dushoff, C.-Y. Leung, G. Li, A. Măgălie, S. W. Park, R. Rodriguez-Gonzalez, S. Shivam, C. Y. Zhao, Modeling shield immunity to reduce COVID-19 epidemic spread. *Nat. Med.* **26**, 849–854 (2020). doi:10.1038/s41591-020-0895-3 Medline

27. J. Wallinga, P. Teunis, M. Kretzschmar, Using data on social contacts to estimate age-specific transmission parameters for respiratory-spread infectious agents. *Am. J. Epidemiol.* **164**, 936–944 (2006). doi:10.1093/aje/kwj317 Medline

28. J. Zhang, M. Litvinova, Y. Liang, Y. Wang, W. Wang, S. Zhao, Q. Wu, S. Merler, C. Viboud, A. Vespignani, M. Ajelli, H. Yu, Changes in contact patterns shape the dynamics of the COVID-19 outbreak in China. *Science* **368**, 1481–1486 (2020). doi:10.1126/science.abb8001 Medline

29. C. M. Saad-Roy, C. E. Wagner, R. E. Baker, S. E. Morris, J. Farrar, A. L. Graham, S. A. Levin, M. J. Mina, C. J. E. Metcalf, B. T. Grenfell, Immune life history, vaccination, and the dynamics of SARS-CoV-2 over the next 5 years. *Science* **370**, 811–818 (2020). doi:10.1126/science.abd7343 Medline

30. X. He, E. H. Y. Lau, P. Wu, X. Deng, J. Wang, X. Hao, Y. C. Lau, J. Y. Wong, Y. Guan, X. Tan, X. Mo, Y. Chen, B. Liao, W. Chen, F. Hu, Q. Zhang, M. Zhong, Y. Wu, L. Zhao, F. Zhang, B. J. Cowling, F. Li, G. M. Leung, Temporal dynamics in viral shedding and transmissibility of COVID-19. *Nat. Med.* **26**, 672–675 (2020). doi:10.1038/s41591-020-0869-5 Medline

31. S. Sanche, Y. T. Lin, C. Xu, E. Romero-Severson, N. Hengartner, R. Ke, High contagiousness and rapid spread of severe acute respiratory syndrome coronavirus 2. *Emerg. Infect. Dis.* **26**, 1470–1477 (2020). doi:10.3201/eid2607.200282 Medline

32. S. M. Kissler, C. Tedijanto, E. Goldstein, Y. H. Grad, M. Lipsitch, Projecting the transmission dynamics of SARS-CoV-2 through the postpandemic period. *Science* **368**, 860–868 (2020). doi:10.1126/science.abb5793 Medline

33. M. Chan-Yeung, R.-H. Xu, SARS: Epidemiology. *Respirology* **8** (suppl.), S9–S14 (2003). doi:10.1046/j.1440-1843.2003.00518.x Medline

34. R. Verity, L. C. Okell, I. Dorigatti, P. Winskill, C. Whittaker, N. Imai, G. Cuomo-Dannenburg, H. Thompson, P. G. T. Walker, H. Fu, A. Dighe, J. T. Griffin, M. Baguelin, S. Bhatia, A. Boonyasiri, A. Cori, Z. Cucunubá, R. FitzJohn, K. Gaythorpe, W. Green, A. Hamlet, W. Hinsley, D. Laydon, G. Nedjati-Gilani, S. Riley, S. van Elsland, E. Volz, H. Wang, Y. Wang, X. Xi, C. A. Donnelly, A. C. Ghani, N. M. Ferguson, Estimates of the severity of coronavirus disease 2019: A model-based analysis. *Lancet Infect. Dis.* **20**, 669–677 (2020). doi:10.1016/S1473-3099(20)30243-7 Medline

35. J. S. Lavine, COVID Immunity and Endemicity Code, Version 1.0.0, Zenodo (2020); https://doi.org/10.5281/zenodo.4390505.

36. H. W. Schroeder Jr., L. Cavacini, Structure and function of immunoglobulins. *J. Allergy Clin. Immunol.* **125** (suppl. 2), S41–S52 (2010). doi:10.1016/j.jaci.2009.09.046 Medline

37. A. T. Huang, B. Garcia-Carreras, M. D. T. Hitchings, B. Yang, L. C. Katzelnick, S. M. Rattigan, B. A. Borgert, C. A. Moreno, B. D. Solomon, L. Trimmer-Smith, V. Etienne, I. Rodriguez-Barraquer, J. Lessler, H. Salje, D. S. Burke, A. Wesolowski, D. A. T. Cummings, A systematic review of antibody mediated immunity to coronaviruses: kinetics, correlates of protection, and association with severity. *Nat. Commun.* **11**, 4704 (2020). doi:10.1038/s41467-020-18450-4 Medline

38. D. A. Griffiths, A catalytic model of infection for measles. *Appl. Stat.* **23**, 330–339 (1974). doi:10.2307/2347126

39. L.-P. Wu, N.-C. Wang, Y.-H. Chang, X.-Y. Tian, D.-Y. Na, L.-Y. Zhang, L. Zheng, T. Lan, L.-F. Wang, G.-D. Liang, Duration of antibody responses after severe acute respiratory syndrome. *Emerg. Infect. Dis.* **13**, 1562–1564 (2007). doi:10.3201/eid1310.070576 Medline

40. National Center for Health Statistics, Mortality in the United States, 2018; www.cdc.gov/nchs/data/databriefs/db355_tables-508.pdf#page=3%202018%20data.

41. L. M. Howden, J. A. Meyer, Age and sex composition: 2010: 2010 census briefs (Report no. C2010BR-03, U.S. Department of Commerce, Economics and Statistics Administration, U.S. Census Bureau, 2011); www.census.gov/prod/cen2010/briefs/c2010br-03.pdf.

42. D. M. Patrick, M. Petric, D. M. Skowronski, R. Guasparini, T. F. Booth, M. Krajden, P. McGeer, N. Bastien, L. Gustafson, J. Dubord, D. Macdonald, S. T. David, L. F. Srour, R. Parker, A. Andonov, J. Isaac-Renton, N. Loewen, G. McNabb, A. McNabb, S.-H. Goh, S. Henwick, C. Astell, J. P. Guo, M. Drebot, R. Tellier, F. Plummer, R. C. Brunham, An outbreak of human coronavirus OC43 infection and serological cross-reactivity with SARS coronavirus. *Can. J. Infect. Dis. Med. Microbiol.* **17**, 330–336 (2006). doi:10.1155/2006/152612 Medline